DOI: 10.1002/ejic.200900307

Synthesis, Structures, and Excited-State Geometries of Alkynylgold(I) Complexes

Lei Gao,[a] David V. Partyka,[b] James B. Updegraff III,[a] Nihal Deligonul,[a] and Thomas G. Gray*[a]

Keywords: Gold / Alkynyl complexes / Luminescence / Triplet states / Density-functional theory

A series of phosphane- and (N-heterocyclic carbene)gold(I) complexes were prepared by deprotonation of terminal alkyne precursors and reaction with the corresponding gold(I) chlorides. Some ten new compounds are reported; these are characterized by multinuclear NMR, optical spectroscopy, and elemental analysis. Crystallographic characterization is reported for five complexes. Organogold species bearing conjugated aryl substituents on the alkynyl ligand are luminescent. Density-functional theory calculations on a model complex suggest that emission and the first several absorption transitions result from excited states dominated by the arylacetylide ligand. Excited-state geometry optimization finds that the lowest-energy triplet state bears linear, two-coordinate gold(I) with a miniscule lengthening of the alkynyl carbon–carbon bond. An unusual triplet excited state having a bent geometry at gold lies at higher energy in arylacetylide complexes. For the model terminal acetylide $Me_3PAuC{\equiv}CH$, the calculations find this bent state to be the lowest-energy triplet.

Introduction

The family of alkynylgold(I) complexes is varied and its history is long.[1–3] In 1866, Berthelot reported the explosive gold carbide Au_2C_2, which precipitates when acetylene gas reacts with solutions of a gold salt.[4] Today, complexes of the type (L)AuC≡CR constitute a majority of gold(I) alkynyls; L may be an organophosphane ligand, an N-heterocyclic carbene ligand, or even the ammonia molecule.[5] The predominant structural feature of gold(I) alkynyls is the two-coordinate, linear binding geometry about gold. This, together with the linearity of the carbon–carbon triple bond imparts a rigid-rod topology of the (alkynyl)gold(I) moiety. Accordingly, gold(I) alkynyls find use as supramolecular synthons,[6–10] notably in the preparation of catenanes.[11,12] Multinuclear gold(I) complexes, including dendrimers,[13] are obtainable from organic precursors bearing several terminal alkyne functionalities. The rod-like character of (alkynyl)gold complexes has also prompted investigation of liquid-crystalline behavior.[14,15]

Much current interest in (alkynyl)gold(I) species derives from their luminescence capabilities. Emission most often results from inter- or intramolecular interactions between gold(I) centers (aurophilicity),[16–23] or from the triplet excited-state manifold of the alkynyl ligand itself. The spin-orbit coupling constant of a gold 5d-electron ($5100\ cm^{-1}$)[24] is comparable to that of a 5p-electron in iodine ($5700\ cm^{-1}$).[25,26] This heavy-atom effect intermingles singlet and triplet excited-states, relaxes spin-selection rules, and opens access to the ligands' triplet-state manifolds.[27–32] Solution-phase luminescence responds to remote perturbations. For example, gold(I) alkynyls bearing pendant crown ether- or calixarene moieties[33–35] are cation sensors, some with selectivity for potassium over sodium in dichloromethane/methanol mixtures.[36]

Luminescence of gold(I) alkynyls in the solid state is typically ligand-centered if metallophilic interactions are suppressed, say with encumbering ligands such as tricyclohexylphosphane. Excitonic coupling still occurs in crystalline solids and depends on the relative orientation of molecules within the unit cell.[37,38]

The chemical reactivity of the gold-bound carbon–carbon triple bond has been relatively under-explored. Recent work from this laboratory has shown[39] that phosphanegold(I) alkynyls react with hydrozoic acid equivalents under mild conditions to yield triazolate products. In these compounds, gold binds a monoanionic triazolate ligand through carbon. The same complexes are preparable by reacting terminal alkynes with the corresponding phosphanegold(I) azide reagent, although in somewhat attenuated yields.

Our investigations of gold(I) triazolates have produced a family of new (alkynyl)gold(I) complexes; several are luminescent. Ten new gold alkynyl compounds are disclosed

[a] Department of Chemistry, Case Western Reserve University, Cleveland, Ohio 44106, USA
E-mail: tgray@case.edu
[b] Creative Chemistry, LLC, Cleveland, Ohio 44106, USA
Supporting information for this article is available on the WWW under http://dx.doi.org/10.1002/ejic.200900307.

here; five are crystallographically characterized. The syntheses, structures, and spectroscopic attributes of the new compounds are discussed.

Scheme 1 enumerates new compounds.

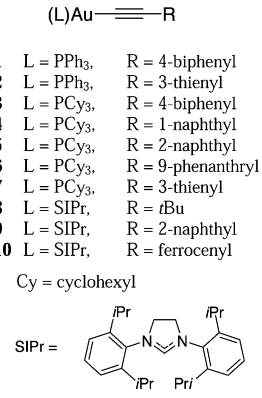

Scheme 1. Designation of compounds.

Results and Discussion

Syntheses

Preparation of the new gold(I) alkynyl compounds relies on the in situ deprotonation of terminal alkynes with sodium- or potassium *tert*-butoxide in methanol, as in previous work.[40–43] Scheme 2 depicts a representative synthesis, of 9-ethynylphenanthryl complex **6**. Methanol solutions of the alkali metal acetylides are added to suspensions of the phosphane- or (N-heterocyclic carbene)gold(I) chloride. Washing with cold methanol, followed by extraction into dichloromethane and solvent removal, affords the phosphanegold(I) acetylide products. Methanol-soluble (N-heterocyclic carbene)gold(I) acetylide products were isolated by removing methanol, extracting into ether and evaporating the solvent. The compounds so obtained are frequently analytically pure; however, contamination with the gold(I) chloride reagents occasionally occurs. In these instances, vapor diffusion of pentane into benzene solutions yields the analytically pure product.

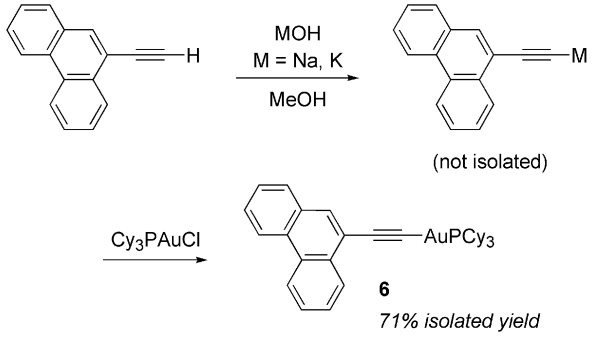

Scheme 2.

Structures

Compounds **1**, **3**, **5**, **9**, and **10** afforded X-ray quality crystals upon vapor diffusion of pentane into concentrated benzene solutions. Thermal ellipsoid projections of two typical compounds, **5** and **10**, appear in Figure 1; those for other crystallographically characterized compounds constitute Figures S1–S3 of the Supporting Information. Table 1 collects crystallographic data for gold(I) alkynyl compounds. No structure shows imposed crystallographic symmetry. Table 2 and Table 3 summarize metric parameters involving gold and the carbon–carbon triple bond. Phosphorus–gold bond lengths range from 2.2632(10) Å in **1** to 2.3009(5) Å in one independent molecule of **3**. The two gold-carbene carbon distances are 1.999(3) Å and 2.0132(19) Å in **9** and **10**, respectively. The span of gold-alkynyl carbon bond lengths is 1.988(2) Å for **10** to 2.024(4) Å in **5**. These gold(I) donor atom bond lengths fall within normal ranges.[44–53] Carbon–carbon triple bond lengths range from 1.162(5) Å for **5** to 1.205(3) Å for one independent molecule of **3**. These C≡C bond lengths are similar to those encountered in a cationic, π-bound gold(I) *alkyne* complex [1.221(8) Å][54] and in neutral (3-hexyne)-AuCl (1.224(6) Å].[55,56]

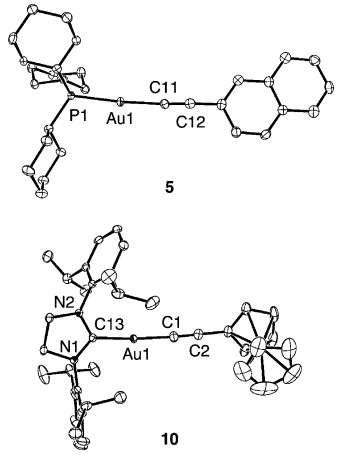

Figure 1. Thermal ellipsoid projections of **5** and **10** (100 K, 50% probability). A partial numbering system is indicated. Hydrogen atoms are omitted for clarity.

The bond angles of Table 3 show the Au–C≡C–R linkages to be essentially linear. The available crystal structures show no close approaches between gold(I) centers, nor is there obvious π-stacking.

Optical Spectroscopy

Alkynyl complexes having polycyclic aromatic hydrocarbyl fragments are luminescent in fluid solvents at room temperature. Table 4 collects luminescence maxima of emissive compounds. All emission profiles show vibronic structure, and dual emission occurs in several cases.

Phenanthryl acetylide complex **6** is representative. Absorption and emission spectra of this compound in THF solvent appear in Figure 2. Absorption sets in near 350 nm. Maxima occur at 331 and 316 nm, with an absorption shoulder near 305 nm. Shorter-wavelength absorption maxima occur between 250–300 nm.

Table 1. Crystallographic data for alkynylgold(I) complexes.

	1	**3**	**5**	**9**	**10**
Formula	$C_{32}H_{24}AuP$	$C_{32}H_{42}AuP$	$C_{30}H_{40}AuP$	$C_{39}H_{45}AuN_2$	$C_{39}H_{47}AuFeN_2$
Fw	636.45	654.59	628.56	738.74	796.60
Crystal system	triclinic	monoclinic	monoclinic	monoclinic	orthorhombic
Space group	$P\bar{1}$	$P2_1/n$	$P2_1/c$	$P2_1$	$P2_12_12_1$
a [Å]	9.995(4)	13.1222(8)	12.289(4)	12.8343(10)	12.2581(8)
b [Å]	12.350(4)	16.9075(11)	17.142(5)	10.3083(8)	14.5555(9)
c [Å]	12.508(7)	25.0523(16)	12.301(4)	15.8854(13)	19.8593(12)
α [deg]	100.358(4)	–	–	–	–
β [deg]	111.113(5)	95.310(1)	93.976(2)	113.7940(10)	–
γ [deg]	113.341(3)	–	–	–	–
Cell volume [Å]^3)	1225.0(9)	5534.3(6)	2585.0(1)	1923.0(3	3543.4(4)
Z	2	8	4	2	4
$D_{calcd.}$ [Mg/m^3]	1.725	1.571	1.615	1.276	1.493
T [K]	100(2)	100(2)	296(2)	100(2)	100(2)
μ [mm^{-1}]	6.088	5.392	5.769	3.850	4.573
F(000)	620	2624	1256	744	1600
Cryst size [mm^3]	$0.28 \times 0.17 \times 0.11$	$0.55 \times 0.35 \times 0.14$	$0.15 \times 0.10 \times 0.06$	$0.34 \times 0.27 \times 0.26$	$0.39 \times 0.30 \times 0.27$
θ_{min}, θ_{max}, [deg]	1.94, 27.00	1.45, 28.05	2.04, 27.28	1.73, 26.86	1.73, 27.93
No. of reflections collected	13803	66274	29711	21070	42076
No. of independent reflections	5063	13204	4859	8077	8327
No. of refined parameters	403	613	289	387	396
Goodness-of-fit on F^2[a]	1.155	0.998	1.038	1.036	1.003
Final *R* indices[b] [$I > 2\sigma(I)$], R_1	0.0165	0.0180	0.0274	0.0241	0.0144
wR_2	0.0174	0.0217	0.0371	0.0579	0.0373
R indices (all data), R_1	0.0483	0.0434	0.0624	0.0253	0.0154
wR_2	0.0487	0.0451	0.0661	0.0582	0.0375

[a] GOF = $[\Sigma w(F_o^2 - F_c^2)^2/(n-p)]^{1/2}$; *n* = number of reflections, *p* = number of parameters refined. [b] $R_1 = \Sigma(||F_o| - |F_c||)/\Sigma|F_o|$; $wR_2 = [\Sigma w(F_o^2 - F_c^2)^2/\Sigma wF_o^4]^{1/2}$.

Table 2. Selected interatomic distances [Å] in crystallographically characterized gold(I) complexes.

Compound	Au–P	Au–$C_{carbene}$	Au–$C_{alkynyl}$	C≡C
1	2.2632(10)		1.991(3)	1.191(4)
3	2.3009(5), 2.2870(5)		2.0177(19), 2.011(2)	1.205(3), 1.190(3)
5	2.2800(10)		2.024(4)	1.162(5)
9		1.999(3)	1.994(4)	1.171(5)
10		2.0132(19)	1.988(2)	1.204(3)

Table 3. Selected interatomic angles [°].[a]

Compound	∠P–**Au**–C_{alkyne}	∠$C_{carbene}$–**Au**–C_{alkyne}	∠Au–**C**≡C	∠C≡**C**–R
1	174.51(8)		170.9(3)	178.0(3)
3	178.62(5), 174.94(6)		178.44(18), 177.14(18)	178.5(2), 176.2(2)
5	175.14(10)		176.0(4)	177.1(4)
9		179.4(5)	175.0(10)	176.3(7)
10		174.23(8)	172.45(19)	175.8(3)

[a] The atom symbols printed in boldface type lies at the vertex of the angle.

Table 4. Luminescence maxima (273 ± 2 K) of emissive compounds in THF solution. Excitation wavelengths λ_{ex} are indicated.

Compound	λ_{ex} [nm]	E_{em} [nm]
1	310	331, 353, 497, 533
3	310	330, 345, 497, 533
4	285	305, 319, 533, 579
5	310	343, 359, 501, 540, 583
6	330	366, 385, 406, 529, 577
9	314	346, 362, 503, 542, 586

An emission, assigned as an ethynylphenanthryl-centered singlet state, commences at ca. 350 nm, with vibronic maxima at 366, 385, and 406 nm. The average peak-to-peak spacing, 1480 cm^{-1}, suggests activation of ring-deforming vibrations. The small Stokes shift indicates singlet parentage of this structured emission. Free 9-ethynylphenanthrene displays a single, structured emission extending from 330–475 nm that maximizes at 376 nm, Supporting Information, Figure S4. Its absorption onset is blue-shifted relative to that of **6**; the first absorption peak occurs at 313 nm.

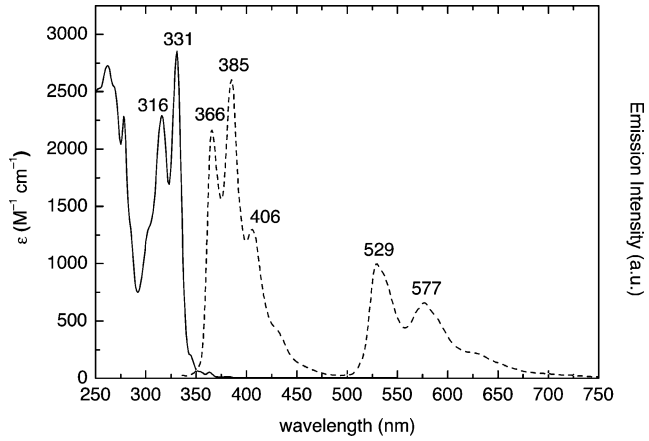

Figure 2. Room-temperature absorption (solid) and emission (dashed) of 9-ethynylphenanthryl complex **6** in THF. Local absorption maxima are indicated.

For gold complex **6**, a second vibronically structured emission appears from 510–650 nm. No corresponding emission is evident in the spectrum of the free alkyne. The Stokes shift of this luminescence is ca. 11 000 cm^{-1}. This lower-energy emission is quenched on exposure to oxygen, and is assigned as an ethynylphenanthryl-centered triplet state. These observations invite computational study.

Computations

Quantum-chemical calculations have been undertaken on model complexes to investigate the electronic structure of the new alkynylgold(I) compounds. Alkynyl **6′** is a simplified analogue of alkynyl **6**, where methyl groups substitute for phosphane cyclohexyl groups. The geometry of the singlet ground state and the first triplet excited state were optimized for **6′**. Harmonic frequency calculations affirm the converged structures to be potential energy minima.

Optimized metrics for **6′** agree favorably with the crystallographic geometry of **6**. The calculated structure possesses C_s symmetry. The carbon–gold bond length, calculated at 1.998 Å is similar to those assembled in Table 2. The alkynyl carbon–carbon triple bond length is calculated to be 1.230 Å, 0.036 Å longer than the mean of those in Table 2. The optimized structure reproduces the linearity about gold with a calculated C–Au–P bond angle of 179.94°.

Figure 3 depicts a partial Kohn–Sham orbital energy-level diagram of **6′**. Plots of frontier orbitals appear at the right. The highest-occupied Kohn–Sham orbital (HOMO) and the lowest unoccupied Kohn–Sham orbital (LUMO) are mainly centered on the arylacetylide ligand, as are the HOMO – 1 and the LUMO + 1. Figure 3 indicates compositions[57] of the frontier orbitals in terms of percentages of phosphanegold(I) and arylacetylide fragment density. Among the occupied orbitals within the energy interval of Figure 3, only the HOMO–4 is metal-localized. This orbital overlaps with the sp-hybrid orbital of the adjacent alkynyl carbon atom.

The HOMO and LUMO bear significant contributions from the alkyne triple bond. The HOMO is 26.9% composed of alkynyl electron density. This alkynyl π-bonding orbital is conjugated into the phenanthryl π-cloud, and the phenanthryl contribution to the HOMO is 68.6%. The LUMO carries 12.0% alkynyl character (79.9% phenanthryl). Alkynyl contributions to the HOMO – 1 and the LUMO + 1 are negligible.

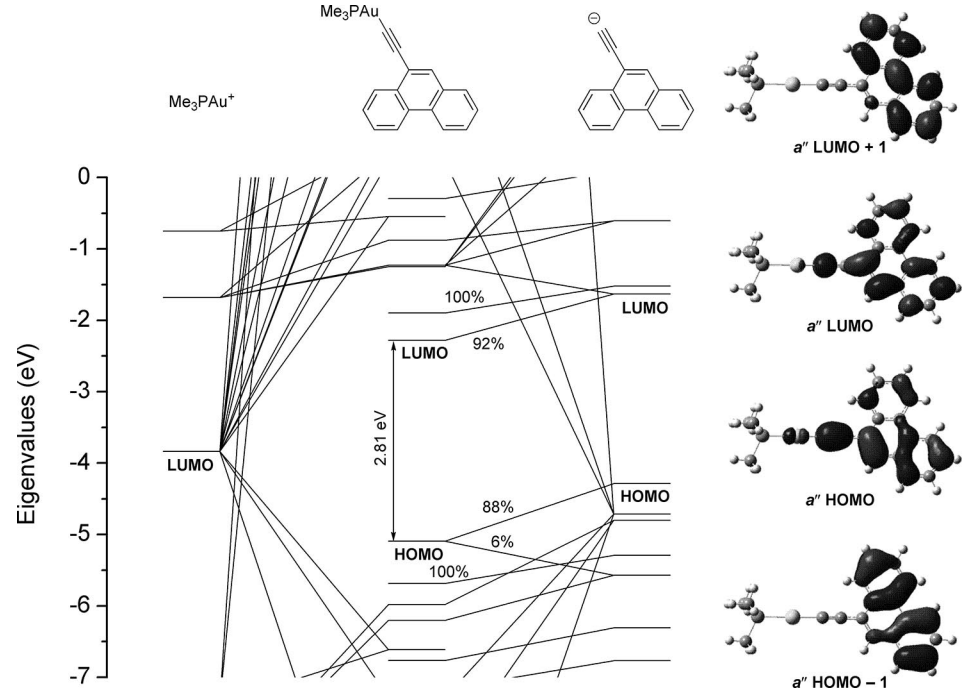

Figure 3. Partial energy level diagram of model compound **6′** (mpmpw91/Stuttgart ECP and basis on Au); implicit THF solvation is included through a polarizable continuum model. Right: plots of selected orbitals (contour level 0.03 a.u.).

Time-dependent density-functional theory (TDDFT) calculations on **6′** find that its first few singlet-singlet transitions are promotions to A′ states that intermingle through configuration interaction. (All spin-allowed transitions are optically permitted in C_s symmetry.) The first optically allowed transition is calculated at 378.71 nm in continuum THF with an oscillator strength of 0.1216. A second, more intense transition is calculated at 372.44 nm; its oscillator strength is 0.4733. The next spin-allowed transition is calculated at 333.68 nm. These calculated absorptions are in fair agreement with the absorption onset for **6** in THF. Two triplet states are calculated to lie below the first excited singlet (calculated for the optimized geometry of ground-state **6′**). The lowest-lying of these, corresponding to the triplet-state emission, is a LUMO→HOMO transition. Its calculated wavelength, 665.80 nm, is in poor agreement with the triplet emission observed at 529 nm.

Triplet State Geometries: The geometry of the lowest triplet state of **6′** was optimized in a spin-unrestricted computation. Energy-minimization proceeded without imposed symmetry, and a harmonic frequency calculation finds the optimized structure to be a minimum of the potential energy hypersurface. For comparison, triplet-state optimizations were also carried out on the terminal gold acetylide ^{3}[Me_3PAu–C≡CH] and on phenylacetylide complex ^{3}[Me_3PAu–C≡CPh].

Triplet-state geometries of ^{3}[Me_3PAu–C≡CPh] and ^{3}**6′** appear in Figure 4, along with selected calculated metrics. The lowest-energy triplets of Me_3PAu–C≡CPh and **6′** retain linear geometries about gold. Carbon–gold and phosphorus–gold bond lengths change little on reaching the triplet state. In both cases, the alkynyl C≡C bond distends in the triplet, owing to the promotion of a π-bonding electron to a π* orbital. The C≡C bond lengthening lessens as conjugation of the arylacetylide ligand increases; the promoted electron is delocalized throughout the carbocyclic π-system.

Metal-Centered Triplet States: An unrestricted geometry optimization of ^{3}[Me_3PAu–C≡CH] converged to the triplet structure depicted in part (a) of Figure 5. This entity is a gold-centered triplet state, in contrast to the ligand-centered triplets encountered for arylacetylide complexes. A ligand-centered triplet structure has also been located; it appears in Figure 5 (b). In the gas-phase, this ligand-centered triplet is 8.22 kcal mol^{-1} more energetic (based on sums of electronic and thermal free energies) than its metal-centered counterpart. The promoted electron resides in an acetylide π* orbital, and partial rehybridization at carbon occurs. Figure 5 depicts the higher-energy singly occupied orbitals of the triplet states of Me_3PAu–C≡CH, each below its respective structure.

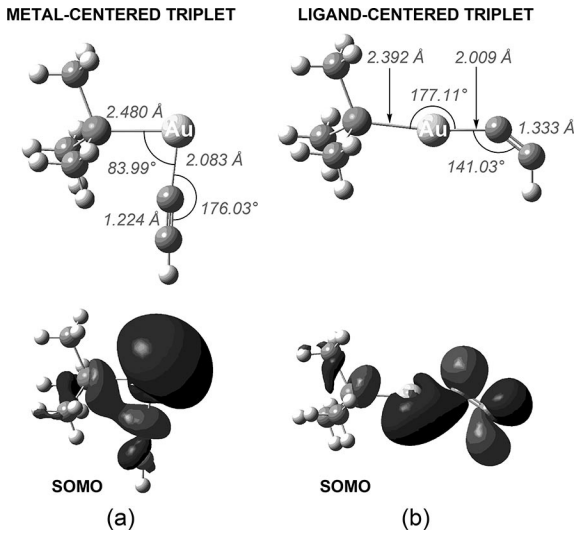

Figure 5. Top: optimized structures of two triplet states of model compound Me_3PAu–C≡CH; structure (a) has lower energy. Selected metrics are indicated. Bottom: the higher-energy singly occupied Kohn–Sham orbitals (SOMOs); contour level 0.03 a.u.

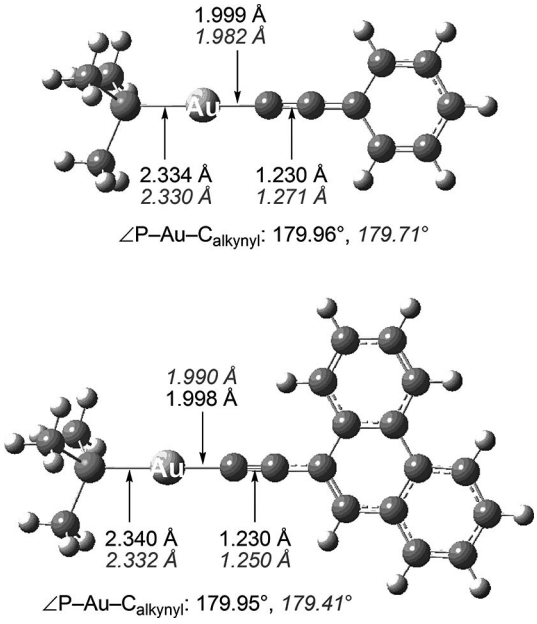

Figure 4. Calculated geometries of the lowest-lying triplet states of model complexes Me_3PAu–C≡CPh and **6′**. Excited-state metrics are non-italicized; triplet states are in italics.

In the metal-centered triplet states a gold-based orbital is populated that has antibonding character toward phosphorus and the acetylide carbon atom. Gold, with its bent two-coordination, is describable as sd-hybridized.[58] Similar gold-centered triplet excited states were also found for ^{3}[Me_3PAu–C≡CPh] and ^{3}**6′**. In these complexes, the metal-centered triplets lie higher in energy than do the ligand-based triplet states. Depictions of these metal-centered triplet geometries appear in Figure S5, Supporting Information. These bent triplet structures are local energy minima, as found from harmonic frequency calculations. Figure 6 plots relative energies of metal- and ligand-centered triplet states for terminal, phenyl-, and (9-phenanthryl-ethynyl)gold(I) complexes. The ligand-based triplet state stabilizes as conjugation of the alkynyl ligand increases.

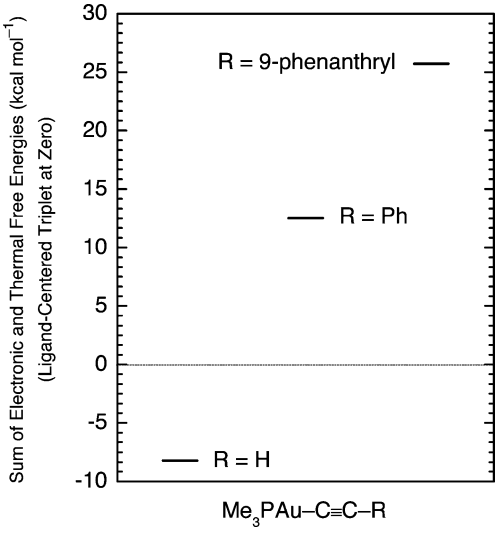

Figure 6. Energies of metal-centered triplet states relative to the corresponding ligand-based triplet. Differences in sums of electronic and thermal free energies are indicated.

Conclusions

The principal results and conclusions of this investigation are as follows.

(1) Phosphane- and (N-heterocyclic carbene)gold(I) alkynyl complexes were prepared by deprotonation of terminal alkynes in situ, followed by reaction with chloridogold(I) complexes. Isolated yields as high as 91% are realized.

(2) Five new compounds have been crystallographically characterized. Close gold–gold interactions (aurophilic attractions) are absent, presumably because of steric heft about the supporting phosphane and carbene ligands.

(3) Gold(I) arylacetylide complexes luminesce at room temperature. Dual, structured emission is observed. The longer-wavelength emission is oxygen-quenchable, and is attributed to arylacetylide ligand fluorescence. Shorter-wavelength emissions are assigned as the corresponding singlet-state fluorescence. The longer-wavelength triplet emission is not observed for the parent (non-metallated) alkyne under identical conditions.

(4) Density-functional theory calculations of the model complex Me_3PAu(9-ethynylphenanthryl), **6′**, find its frontier orbitals to lie almost entirely on the arylacetylide ligands. Gold(I) is a nonchromophoric spectator.

(5) Optimization of the lowest-lying triplet state of **6′** and of ^{3}[Me_3PAu–C≡CPh] preserves the linear geometry about gold. The ground-state carbon–carbon triple bond lengthens in the exited state ca. 0.04 Å for ^{3}[Me_3PAu–C≡CPh] and ca. 0.02 Å for ^{3}**6′**. Greater delocalization of the promoted electron in the ethynylphenanthryl complex lessens the local alkynyl distortion, despite population of a nominally C≡C π* orbital.

(6) Geometry optimization has also located triplet excited states with a ca. 90° bent geometry about gold, for Me_3PAu–C≡CH, Me_3PAu–C≡CPh, and **6′**. This bent triplet state is the lowest-energy triplet for the terminal alkynyl complex Me_3PAu–C≡CH. A second triplet state lies some 8.2 kcal mol^{-1} higher in energy. In this state, the promoted electron occupies a C≡C π* orbital. The alkynyl carbon–carbon bond stretches to 1.333 Å, compared to 1.223 Å in the ground state. Extensive rehybridization of the alkynyl carbon atoms occurs (Figure 5).

(7) Bent, metal-centered triplet states have been located for the model arylacetylide complexes Me_3PAu–C≡CPh, and **6′**. However, these have higher energies than the foregoing ligand-centered triplets. By Kasha's rule,[59,60] the observed phosphorescence is expected to derive from the first triplet state.

Research in this laboratory continues to elaborate the ligand-centered transformations of gold(I) alkynyl compounds and the photophysics of gold compounds. These studies are ongoing.

Experimental Section

General: All solvents and reagents were used as received. (PCy_3)AuCl and (PPh_3)AuCl were synthesized by a slight modification of the literature procedures (used toluene and Au(tht)Cl).[61] (SIPr)AuCl was made according to the literature procedure.[62] Procedures for alkynylgold(I) complexes were done in air. Microanalyses (C, H, N) were performed by Robertson Microlit Laboratories, Inc. NMR spectra (^{1}H and ^{31}P{^{1}H}) were recorded with a Varian AS-400 spectrometer operating at 399.7 and 161.8 MHz respectively. For ^{1}H NMR spectra, chemical shifts were determined relative to the solvent residual peaks. For ^{31}P{^{1}H} NMR spectra, chemicals shifts were determined relative to concentrated H_3PO_4.

General Procedure for New Alkynylgold(I) (Species): *tert*-Butoxide was dissolved in ca. 4 mL of MeOH, sodium (or potassium), and 1 equiv. of the appropriate alkyne was added to this solution. The suspension was mixed until it was a solution and then further mixed for 5–10 min. The solution was added to a suspension of LAuCl (0.50–0.60 equiv.; L = PPh_3, PCy_3, SIPr) and stirred for 1–2 h (for phosphane derivatives) or overnight (for SIPr derivatives).

The phosphane derivatives were collected by filtration, washed with cold methanol and pentane, extracted with dichloromethane, filtered, and the solvent was removed by use of a rotary evaporator. The resultant residue was triturated with pentane and the solid collected. In most cases, the as-isolated solid was pure with perhaps a *trace* of (PR_3)AuCl remaining, but recrystallized yields (which are reported unless otherwise stated) via benzene/pentane vapor diffusion gave analytically pure material.

For carbene complexes, the solvent was removed from the resultant solution, and the solid left was extracted with diethyl ether and filtered. The solvent was removed from the filtrate, and pentane trituration yielded the products as powders. Benzene/pentane vapor diffusion yielded analytically pure crystals.

[(PPh_3)Au(4-biphenylethynyl)] (1): KO*t*Bu (46 mg, 0.41 mmol), 4-ethynylbiphenyl (72 mg, 0.41 mmol), and (PPh_3)AuCl (102 mg, 0.21 mmol). No recrystallization of the product was required. Yield 101 mg (78%). ^{1}H NMR (C_6D_6): δ = 7.89 (d, J = 8.4 Hz, 2 H, 4-biphenylethynyl), 7.38 (d, J = 7.2 Hz, 2 H, 4-biphenylethynyl), 7.33 (d, J = 8.0 Hz, 2 H, 4-biphenylethynyl), 7.20–7.30 (m, 6 H), 7.15–7.19 (m, 2 H), 7.08 (t, J = 7.2 Hz, 1 H, 4-biphenylethynyl), 6.84–6.98 (m, 9 H) ppm. ^{31}P{^{1}H} NMR (C_6D_6): δ = 42.6 (s) ppm. IR (KBr): $\tilde{\nu}$ = 2109 (w, $\upsilon_{C\equiv C}$) cm^{-1}. UV/Vis (THF): λ (ε, M^{-1}cm^{-1}) = 284 (38400), 296 (42200), 309 (36900) nm. $C_{32}H_{24}AuP$ (636.48): calcd. C 60.39, H 3.80; found C 60.51, H 3.95.

[(PPh$_3$)Au(3-thienylethynyl)] (2): KO*t*Bu (90 mg, 0.9 mmol), 3-ethynylthiophene (88.5 mg, 0.8 mmol) and PPh$_3$AuCl (282 mg, 0.6 mmol). Yield 251 mg (91%). ^{1}H NMR (C_6D_6): δ = 7.36 (d, J = 2.8 Hz, 1 H, 3-thienyl), 7.31 (d, J = 4.8 Hz, 1 H, 3-thienyl), 7.22 (dd, J = 12.4, 7.2 Hz, 6 H, ($C_{18}H_{15}$)P), 6.85–6.96 (m, 9 H, ($C_{18}H_{15}$)-P), 6.72 (dd, J = 4.8, 2.8 Hz, 1 H, 3-thienyl) ppm. ^{31}P{^{1}H} NMR (C_6D_6): δ = 42.4 ppm. IR (KBr): $\tilde{\nu}$ = 2110 (w, $\upsilon_{C\equiv C}$) cm^{-1}. $C_{24}H_{18}AuPS$ (566.41): calcd. C 50.89, H 3.20; found C 50.70, H 3.29.

[(PCy$_3$)Au(4-biphenylethynyl)] (3): NaO*t*Bu (49 mg, 0.51 mmol), 4-ethynylbiphenyl (90 mg, 0.50 mmol), and (PCy$_3$)AuCl (133 mg, 0.26 mol). Yield 102 mg (60%). ^{1}H NMR (C_6D_6): δ = 7.83 (d, J = 8.0 Hz, 2 H, 4-ethynylbiphenyl), 7.36 (d, J = 7.6 Hz, 2 H, 4-ethynylbiphenyl), 7.30 (d, J = 8.0 Hz, 2 H, 4-ethynylbiphenyl), 7.13–7.17 (m, 2 H), 7.07 (t, J = 7.2 Hz, 1 H, 4-ethynylbiphenyl), 0.84–1.80 (m, 33 H, C_6H_{11}) ppm. ^{31}P{^{1}H} NMR (C_6D_6): δ = 56.7 (s) ppm. IR (KBr): $\tilde{\nu}$ = 2109 (w, $\upsilon_{C\equiv C}$) cm^{-1}. UV/Vis (THF): λ (ε, M^{-1}cm^{-1}) = 296 (40900), 305 (37600) nm. $C_{32}H_{42}AuP$ (654.62): calcd. C 58.71, H 6.47; found C 58.45, H 6.39.

[(PCy$_3$)Au(1-naphthylethynyl)] (4): KO*t*Bu (37 mg, 0.33 mmol), 1-ethynylnaphthalene (50 mg, 0.33 mmol), and (PCy$_3$)AuCl (84 mg, 0.16 mmol). Yield 66 mg (64%). ^{1}H NMR (C_6D_6): δ = 9.29 (s, J = 8.4 Hz, 1 H, 1-naphthyl), 8.00 (d, J = 6.8 Hz, 1 H, 1-naphthyl), 7.59 (d, J = 8.0 Hz, 1 H, 1-naphthyl), 7.47 (d, J = 8.0 Hz, 1 H, 1-naphthyl), 7.30 (t, J = 7.6 Hz, 1 H, 1-naphthyl), 8.00 (t, J = 7.6 Hz, 1 H, 1-naphthyl), 7.10–7.14 (m, J = 6.8 Hz, 1 H, 1-naphthyl), 0.89–1.80 (m, 33 H, P(C_6H_{11})$_3$) ppm. ^{31}P{^{1}H} NMR (C_6D_6): δ = 56.5 (s) ppm. IR (KBr): $\tilde{\nu}$ = 2107 (w, $\upsilon_{C\equiv C}$) cm^{-1}. UV/Vis (THF): λ (ε, M^{-1}cm^{-1}) = 285 (25300), 300 (21900), 313 (22700), 318 (21700), 332 (23800) nm. $C_{30}H_{40}AuP$ (628.59): calcd. C 57.32, H 6.41; found C 57.48, H 6.21.

[(PCy$_3$)Au(2-naphthylethynyl)] (5): KO*t*Bu (42 mg, 0.37 mmol), 2-ethynylnaphthalene (57 mg, 0.37 mmol), and (PCy$_3$)AuCl (96 mg, 0.19 mmol) and a total of only 4 mL of methanol (2 mL for alkynyl solution, 2 mL for gold suspension). Yield 102 mg (87%). ^{1}H NMR (C_6D_6): δ = 8.26 (s, 1 H, 2-naphthyl), 7.89 (dd, J = 1.6, 8.4 Hz, 1 H, 2-naphthyl), 7.40–7.50 (m, 3 H, 2-naphthyl), 7.09–7.14 (m, 2 H, 2-naphthyl), 0.89–1.80 (m, 33 H, P(C_6H_{11})$_3$) ppm. ^{31}P{^{1}H} NMR (C_6D_6): δ = 56.7 (s) ppm. IR (KBr): $\tilde{\nu}$ = 2109 (w, $\upsilon_{C\equiv C}$) cm^{-1}. UV/Vis (THF): λ (ε, M^{-1}cm^{-1}) 287 (28400), 297 (31000), 311 (33000), 325 (4800), 342 (3000) nm. $C_{30}H_{40}AuP$ (628.59): calcd. C 57.32, H 6.41; found C 57.13, H 6.36.

[(PCy$_3$)Au(9-phenanthrylethynyl)] (6): NaO*t*Bu (45 mg, 0.47 mmol), 2-ethynylphenanthrene (94 mg, 0.47 mmol), and (PCy$_3$)AuCl (119 mg, 0.23 mmol). Yield 111 mg (71%). ^{1}H NMR (C_6D_6): δ = 9.46 (d, J = 7.6 Hz, 1 H, 9-phenanthryl), 8.44 (d, J = 7.6 Hz, 1 H, 9-phenanthryl), 8.38 (d, J = 8.4 Hz, 1 H, 9-phenanthryl), 8.28 (s, 1 H, 9-phenanthryl), 7.46 (q, J = 7.2 Hz, 2 H, 9-phenanthryl), 7.38 (t, J = 7.6 Hz, 1 H, 9-phenanthryl), 7.30 (t, J = 7.2 Hz, 1 H, 9-phenanthryl), 7.23 (t, J = 7.6 Hz, 1 H, 9-phenanthryl), 0.89–1.80 (m, 33 H, P(C_6H_{11})$_3$) ppm. ^{31}P{^{1}H} NMR (C_6D_6): δ = 56.6 (s) ppm. IR (KBr): $\tilde{\nu}$ = 2102 (w, $\upsilon_{C\equiv C}$) cm^{-1}. UV/Vis (THF): λ (ε, M^{-1}cm^{-1}) = 278 (2284), 316 (2291), 331 (2852) nm. $C_{34}H_{42}AuP$ (678.65): calcd. C 60.17, H 6.24; found C 59.89, H 5.99.

[(PCy$_3$)Au(3-thienylethynyl)] (7): KO*t*Bu (56 mg, 0.50 mmol), 3-ethynylthiophene (54 mg, 0.50 mmol), and (PCy$_3$)AuCl (128 mg, 0.25 mmol). The crude material was analytically pure. Yield 115 mg (79%). ^{1}H NMR (C_6D_6): δ = 7.31 (dd, J = 1.2, 2.8 Hz, 1 H, 3-thienyl), 7.27 (dd, J = 1.2, 4.8 Hz, 1 H, 3-thienyl), 6.70 (dd, J = 4.8, 2.8 Hz, 1 H, 3-thienyl), 0.78–1.75 (m, 33 H, P(C_6H_{11})$_3$) ppm. ^{31}P{^{1}H} NMR (C_6D_6): δ = 56.6 (s) ppm. IR (KBr): $\tilde{\nu}$ = 2116 (w, $\upsilon_{C\equiv C}$) cm^{-1}. $C_{24}H_{36}AuPS$ (584.55): calcd. C 49.30, H 6.21; found C 49.49, H 6.30.

[(SIPr)Au(*tert*-butylethynyl)] (8): NaO*t*Bu (100 mg, 1.0 mmol), 3,3-dimethylbut-1-yne (85 mg, 1.0 mmol) and SIPrAuCl (324 mg, 0.5 mmol). Yield 292.4 mg (79%). ^{1}H NMR (C_6D_6): δ = 7.09 (t, J = 7.6 Hz, 2 H, *C*H aromatic on SIPr), 6.97 (d, J = 7.6 Hz, 4 H, *C*H aromatic on SIPr), 3.08 (s, 4 H, *C*H imidazole), 2.94 (sept, J = 6.8 Hz, 4 H, *C*H(CH_3)$_2$), 1.50 (d, J = 6.8 Hz, 12 H, CH(*C*H$_3$)$_2$), 1.15 (s, 9 H, C(*C*H$_3$)$_3$), 1.13 (d, J = 6.8 Hz, 12 H, CH(*C*H$_3$)$_2$) ppm. IR (KBr): $\tilde{\nu}$ = 2110 (w, $\upsilon_{C\equiv C}$) cm^{-1}. $C_{33}H_{47}AuN_2$ (668.71): calcd. C 59.27, H 7.08, N 4.19; found C 59.29, H 7.28, N 4.16.

[(SIPr)Au(2-naphthylethynyl)] (9): NaO*t*Bu (62 mg, 0.6 mmol), 2-ethynylnaphthalene (98.1 mg, 0.6 mmol) and SIPrAuCl (201 mg, 0.3 mmol). Yield 231 mg (79%). ^{1}H NMR (C_6D_6): δ = 7.72 (s, 1 H, 2-naphthyl), 7.39–7.42 (m, 1 H, 2-naphthyl), 7.35–7.37 (m, 1 H, 2-naphthyl), 7.27–7.29 (m, 1 H, 2-naphthyl), 7.18–7.20 (m, 3 H, 2-naphthyl and *C*H aromatic on SIPr), 7.01–7.05 (m, 6 H, 2-naphthyl and *C*H aromatic on SIPr), 3.13 (s, 4 H, *C*H imidazole), 2.99 (sept, J = 6.8 Hz, 4 H, *C*H(CH_3)$_2$), 1.55 (d, J = 6.8 Hz, 12 H, CH(*C*H$_3$)$_2$), 1.17 (d, J = 6.8 Hz, 12 H, CH(*C*H$_3$)$_2$) ppm. IR (KBr): $\tilde{\nu}$ = 2107 (s, $\upsilon_{C\equiv C}$) cm^{-1}. UV/Vis (THF): λ (ε, M^{-1}cm^{-1}) = 262 (48200), 302 (26500), 314 (29700), 343 (5340) nm. $C_{39}H_{45}AuN_2$ (738.76): calcd. C 63.41, H 6.14, N 3.79; found C 63.37, H 5.90, N 3.76.

[(SIPr)Au(ferrocenylethynyl)] (10): NaO*t*Bu (65 mg, 0.68 mmol), 3-ethynylferrocene (141.2 mg, 0.68 mmol) and SIPrAuCl (222 mg, 0.36 mmol). Yield 219 mg (75%). ^{1}H NMR (C_6D_6): δ = 7.12 (t, J = 7.6 Hz, 2 H, *C*H aromatic on SIPr), 7.00 (d, J = 7.6 Hz, *C*H aromatic on SIPr), 4.21, (s, 2 H, ferrocenyl), 3.91 (s, 5 H ferrocenyl), 3.70 (9s, 2 H, ferrocenyl), 3.10 (s, 4 H, *C*H imidazole), 2.95 (sept, J = 6.8 Hz, 4 H, *C*H(CH_3)$_2$), 1.51 (d, J = 6.8 Hz, 12 H, CH(*C*H$_3$)$_2$), 1.15 (s, 9 H, C(*C*H$_3$)$_3$), 1.13 (d, J = 6.8 Hz, 12 H, CH(*C*H$_3$)$_2$) ppm. IR (KBr): $\tilde{\nu}$ = 2102 (w, $\upsilon_{C\equiv C}$) cm^{-1}. UV/Vis (THF): λ (ε, M^{-1}cm^{-1}) = 307 (7250), 449 (248) nm. $C_{39}H_{47}AuFeN_2$ (796.63): calcd. C 58.80, H 5.95, N 3.52; found C 58.89, H 5.85, N 3.49.

X-ray Structure Determination: Products were crystallized by diffusion of pentane into saturated benzene solutions. Single crystal X-ray data were collected with a Bruker AXS SMART APEX II CCD diffractometer using monochromatic Mo-K_α radiation with the omega scan technique. The unit cells were determined using SMART[63] and SAINT+.[64] Data collection for all crystals was conducted at 100 K (–173.5 °C). All structures were solved by direct methods and refined by full-matrix least-squares against F^2 with all reflections using SHELXTL.[65] Refinement of extinction coefficients was found to be insignificant. All non-hydrogen atoms were refined anisotropically. All hydrogen atoms were placed in standard calculated positions and all hydrogen atoms were refined with an isotropic displacement parameter 1.2 times that of the adjacent carbon.

Computations: Spin-restricted density-functional theory computations were performed within the Gaussian 03 program suite.[66] Calculations employed the modified Perdew–Wang exchange functional of Adamo and Barone[67] and the original Perdew–Wang correlation functional.[68] Nonmetal atoms were described with the TZVP basis set of Godbelt, Andzelm, and co-workers.[69] Gold orbitals were described with the Stuttgart effective core potential and the associated basis set,[70] which was contracted as follows: Au, (8s,7p,6d)→[6s,5p,3d]. Relativity with the Stuttgart ECP and its associated basis set is introduced with a potential term (i.e., a one-electron operator) that replaces the two-electron exchange and Coulomb operators resulting from interaction between core elec-

trons and between core and valence electrons. In this way relativistic effects, especially scalar effects, are included implicitly rather than as four-component, one-electron functions in the Dirac equation. Geometries were optimized without imposed symmetry, and harmonic frequency calculations find all structures to be potential energy minima. Calculations on triplet states were spin-unrestricted. Vertical excitation energies were calculated using a TDDFT implementation described by Scuseria and co-workers.[71] All calculated properties reported here include implicit THF solvation (ε = 7.58, 298.15 K), which was incorporated in single-point calculations of the gas-phase geometries with Tomasi's polarizable continuum model (PCM).[72,73] The stability of each converged density was confirmed by calculation of the eigenvalues of the *A* matrix.[74,75] Percentage compositions of molecular orbitals, overlap populations, and bond orders between fragments were calculated using the AOMix program of Gorelsky.[76,77]

Supporting Information (see also the footnote on the first page of this article): Thermal ellipsoid projections of **1**, **3**, and **9**; absorption and emission spectra of free 9-ethynylphenanthrene, optimized Cartesian coordinates of singlet and triplet states of **6′**, Me_3PAu–C≡CH, and Me_3PAu–C≡CPh; crystallographic (CIF) data.

Acknowledgments

The authors thank the U. S. National Science Foundation (NSF) (CHE-0749086, grant to T. G. G.) for support. The diffractometer at Case Western Reserve was funded by an NSF grant (CHE0541766). T. G. G. is an Alfred P. Sloan Foundation Fellow. N. D. holds a Republic of Turkey Ministry of National Education fellowship.

[1] H. Schmidbaur, A. Schier, in: *Comprehensive Organometallic Chemistry III* (Eds.: R. Crabtree, M. Mingos), Elsevier, **2006**, vol. 2, section 2.05.
[2] H. Schmidbaur, in: *Gmelin Handbuch der Anorganischen Chemie*, 8th ed. (Ed.: A. Slawisch), Springer-Verlag, Berlin, **1980**.
[3] H. Schmidbaur, A. Grohmann, M. E. Olmos, in: *Gold: Progress in Chemistry, Biochemistry and Technology* (Ed.: H. Schmidbaur), Wiley, Chichester, **1999**.
[4] M. P. Berthelot, *Justus Liebigs Ann. Chem.* **1866**, *139*, 150.
[5] D. M. P. Mingos, J. Yau, S. Menzer, D. J. Williams, *Angew. Chem. Int. Ed. Engl.* **1995**, *34*, 1894.
[6] J. Vicente, M.-T. Chicote, M. D. Abrisqueta, P. González-Herrero, R. Guerrero, *Gold Bull.* **1998**, *31*, 83.
[7] M. I. Brice, B. C. Hall, B. W. Skelton, M. E. Smith, A. H. White, *J. Chem. Soc., Dalton Trans.* **2002**, 995.
[8] I. O. Koshevoy, A. J. Karttunen, S. P. Tunik, M. Haukka, S. I. Selivanov, A. S. Melnikov, P. Y. Serdobintsev, M. A. Khodorkovskiy, T. A. Pakkanen, *Inorg. Chem.* **2008**, *47*, 9478.
[9] I. O. Koshevoy, Y.-C. Lin, A. J. Karttunen, P.-T. Chou, P. Vainiotalo, S. P. Tunik, M. Haukka, T. A. Pakkanen, *Inorg. Chem.* **2009**, *48*, 2094.
[10] I. O. Koshevoy, A. J. Karttunen, S. P. Tunik, M. Haukka, S. I. Selivanov, A. S. Melnikov, P. Y. Serdobintsev, T. A. Pakkanen, *Organometallics* **2009**, *28*, 1369.
[11] M. J. Irwin, J. J. Vittal, R. J. Puddephatt, *Organometallics* **1997**, *16*, 3541.
[12] N. C. Habermehl, D. J. Eisler, C. W. Kirby, N. L.-S. Yue, R. J. Puddephatt, *Organometallics* **2006**, *25*, 2921.
[13] E. C. Constable, C. E. Housecroft, M. Neuburger, S. Schaffner, E. J. Shardlow, *Dalton Trans.* **2007**, *25*, 2631.
[14] P. Alejos, S. Coco, P. Espinet, *New J. Chem.* **1995**, *19*, 799.
[15] T. Kaharu, R. Ishii, T. Adachi, T. Yoshida, S. Takahashi, *J. Mater. Chem.* **1995**, *5*, 687.
[16] H. Schmidbaur, A. Schier, *Chem. Soc. Rev.* **2008**, *37*, 1931.
[17] H. Schmidbaur, *Gold Bull.* **2000**, *33*, 3.
[18] P. Pyykkö, *Chem. Rev.* **1997**, *97*, 597.
[19] E. M. Gussenhoven, J. C. Fettinger, D. M. Pham, M. A. Malwitz, A. L. Balch, *J. Am. Chem. Soc.* **2005**, *127*, 10838. [Erratum, *J. Am. Chem. Soc.* **2005**, *127*, 16338.].
[20] Y.-A. Lee, R. Eisenberg, *J. Am. Chem. Soc.* **2003**, *125*, 7778.
[21] M. A. Mansour, W. B. Connick, R. J. Lachicotte, H. J. Gysling, R. Eisenberg, *J. Am. Chem. Soc.* **1998**, *120*, 1329.
[22] O. Elbjeirami, M. A. Omary, M. Stender, A. L. Balch, *Dalton Trans.* **2004**, 3173.
[23] S.-L. Zheng, C. L. Nygren, M. Messerschmidt, P. Coppens, *Chem. Commun.* **2006**, 3711.
[24] J. S. Griffith, *The Theory of Transition Metal Ions*, Cambridge University Press, **1964**.
[25] J. Friedrich, F. Metz, F. Dörr, *Mol. Phys.* **1975**, *30*, 289.
[26] A. A. Mohamed, M. A. Rawashdeh-Omary, M. A. Omary, J. P. Fackler Jr., *Dalton Trans.* **2005**, 2597.
[27] T. G. Gray, *Comments, Inorg. Chem.* **2007**, *28*, 181.
[28] K.-L. Cheung, S.-K. Yip, V. W.-W. Yam, *J. Organomet. Chem.* **2004**, *689*, 4451.
[29] O. Elbjeirami, C. N. Burress, F. P. Gabbaï, M. A. Omary, *J. Phys. Chem. C* **2007**, *111*, 9522.
[30] M. R. Haneline, M. Tsunoda, F. P. Gabbaï, *J. Am. Chem. Soc.* **2002**, *124*, 3737.
[31] C. N. Burress, M. I. Bodine, O. Elbjeirami, J. H. Reibenspies, M. A. Omary, F. P. Gabbaï, *Inorg. Chem.* **2007**, *46*, 1388.
[32] A. A. Mohamed, M. A. Rawashdeh-Omary, M. A. Omary, J. P. Fackler Jr., *Dalton Trans.* **2005**, 2597.
[33] X.-X. Lu, C.-K. Li, E. C.-C. Cheng, N. Zhu, V. W.-W. Yam, *Inorg. Chem.* **2004**, *43*, 2225.
[34] V. W.-W. Yam, K.-L. Cheung, L.-H. Yuan, K. M.-C. Wong, K.-K. Cheung, *Chem. Commun.* **2000**, 1513.
[35] S.-K. Yip, E. C.-C. Cheng, L.-H. Yuan, N. Zhu, V. W.-W. Yam, *Angew. Chem. Int. Ed.* **2004**, *43*, 4954.
[36] V. W.-W. Yam, S.-K. Yip, L.-H. Yuan, K.-L. Cheung, N. Zhu, K.-K. Cheung, *Organometallics* **2003**, *22*, 2630.
[37] V. W.-W. Yam, K.-L. Cheung, S.-K. Yip, K.-K. Cheung, *J. Organomet. Chem.* **2003**, *681*, 196.
[38] W. Lu, N. Zhu, C.-M. Che, *J. Am. Chem. Soc.* **2003**, *125*, 16081.
[39] D. V. Partyka, J. B. Updegraff III, M. Zeller, A. D. Hunter, T. G. Gray, *Organometallics* **2007**, *26*, 183.
[40] M. I. Bruce, E. Horn, J. G. Matisons, M. R. Snow, *Aust. J. Chem.* **1984**, *37*, 1163.
[41] R. J. Cross, M. F. Davidson, A. J. McLennan, *J. Organomet. Chem.* **1984**, *265*, C37.
[42] R. J. Cross, M. F. Davidson, *J. Chem. Soc., Dalton Trans.* **1986**, 411.
[43] T. E. Müller, S. W.-K. Choi, D. M. P. Mingos, D. Murphy, D. J. Williams, V. W.-W. Yam, *J. Organomet. Chem.* **1994**, *484*, 209.
[44] J. Strähle, in: *Gold: Progress in Chemistry, Biochemistry and Technology* (Ed.: H. Schmidbaur), Wiley, Chichester, **1999**, p. 311.
[45] J. Vicente, J. Gil-Rubio, N. Barquero, P. G. Jones, D. Bautista, *Organometallics* **2008**, *27*, 646.
[46] V. W.-W. Yam, S.-K. Yip, L.-H. Yuan, K.-L. Cheung, N. Zhu, K.-K. Cheung, *Organometallics* **2003**, *22*, 2630.
[47] V. W.-W. Yam, S. W. K. Choi, *J. Chem. Soc., Dalton Trans.* **1996**, 4227.
[48] G. Jia, N. C. Payne, J. J. Vittal, R. J. Puddephat, *Organometallics* **1993**, *12*, 4771.
[49] T. E. Müller, D. M. P. Mingos, D. J. Williams, *J. Chem. Soc., Chem. Commun.* **1994**, 1787.
[50] V. W.-W. Yam, S. W. K. Choi, K. K. Cheung, *J. Chem. Soc., Dalton Trans.* **1996**, 3411.
[51] R. J. Cross, M. F. Davidson, *J. Chem. Soc., Dalton Trans.* **1986**, 411.
[52] O. M. Abu-Salah, A. R. Al-Ohaly, C. B. Knobler, *J. Chem. Soc., Chem. Commun.* **1985**, 1502.
[53] M. I. Bruce, K. R. Grundy, M. J. Liddell, M. R. Snow, E. R. T. Tiekink, *J. Organomet. Chem.* **1988**, *344*, C49.

[54] N. D. Shapiro, F. D. Toste, *Proc. Natl. Acad. Sci. USA* **2008**, *105*, 2779.
[55] J. Wu, P. Kroll, H. V. R. Dias, *Inorg. Chem.* **2009**, *48*, 423.
[56] Neutral gold(I) π complexes to strained alkynes have also been structurally characterized: P. Schulte, U. Behrens, *Chem. Commun.* **1998**, 1633.
[57] R. S. Mulliken, *J. Chem. Phys.* **1955**, *23*, 1833.
[58] F. Weinhold, C. R. Landis, *Valency and Bonding: A Natural Bond Orbital Donor-Acceptor Perspective*, Cambridge, New York, **2005**, pp. 381.
[59] M. Kasha, *Discuss. Faraday Soc.* **1950**, *9*, 14.
[60] N. J. Turro, *Modern Molecular Photochemistry*; University Science Books, Sausalito, California, **1991**, p. 103.
[61] F. G. Mann, A. F. Wells, D. Purdie, *J. Chem. Soc.* **1937**, 1828.
[62] D. S. Laitar, P. Müller, T. G. Gray, J. P. Sadighi, *Organometallics* **2005**, *24*, 4503.
[63] Bruker Advanced X-ray Solutions, *SMART for WNT/2000* (Version 5.628), Bruker AXS, Inc., Madison, Wisconsin, U.S.A., **1997**–**2002**.
[64] Bruker Advanced X-ray Solutions, *SAINT* (Version 6.45), Bruker AXS, Inc., Madison, Wisconsin, U.S.A., **1997**–2003.
[65] Bruker Advanced X-ray Solutions, *SHELXTL* (Version 6.10), Bruker AXS, Inc., Madison, Wisconsin, U.S.A., **2000**.
[66] M. J. Frisch, G. W. Trucks, H. B. Schlegel, G. E. Scuseria, M. A. Robb, J. R. Cheeseman, J. A. Montgomery Jr., T. Vreven, K. N. Kudin, J. C. Burant, J. M. Millam, S. S. Iyengar, J. Tomasi, V. Barone, B. Mennucci, M. Cossi, G. Scalmani, N. Rega, G. A. Petersson, H. Nakatsuji, M. Hada, M. Ehara, K. Toyota, R. Fukuda, J. Hasegawa, M. Ishida, T. Nakajima, Y. Honda, O. Kitao, H. Nakai, M. Klene, X. Li, J. E. Knox, H. P. Hratchian, J. B. Cross, V. Bakken, C. Adamo, J. Jaramillo, R. Gomperts, R. E. Stratmann, O. Yazyev, A. J. Austin, R. Cammi, C. Pomelli, J. W. Ochterski, P. Y. Ayala, K. Morokuma, G. A. Voth, P. Salvador, J. J. Dannenberg, V. G. Zakrzewski, S. Dapprich, A. D. Daniels, M. C. Strain, O. Farkas, D. K. Malick, A. D. Rabuck, K. Raghavachari, J. B. Foresman, J. V. Ortiz, Q. Cui, A. G. Baboul, S. Clifford, J. Cioslowski, B. B. Stefanov, G. Liu, A. Liashenko, P. Piskorz, I. Komaromi, R. L. Martin, D. J. Fox, T. Keith, M. A. Al-Laham, C. Y. Peng, A. Nanayakkara, M. Challacombe, P. M. W. Gill, B. Johnson, W. Chen, M. W. Wong, C. Gonzalez, J. A. Pople, *Gaussian 03*, Revision D.01, Gaussian, Inc., Wallingford CT, **2004**.
[67] C. Adamo, V. Barone, *J. Chem. Phys.* **1998**, *108*, 664.
[68] J. P. Perdew, Y. Wang, *Phys. Rev. B* **1992**, *45*, 13244.
[69] N. Godbout, D. R. Salahub, J. Andzelm, E. Wimmer, *Can. J. Chem.* **1992**, *70*, 560.
[70] M. Dolg, U. Wedig, H. Stoll, H. Preuss, *J. Chem. Phys.* **1987**, *86*, 866.
[71] R. E. Stratmann, G. E. Scuseria, M. J. Frisch, *J. Chem. Phys.* **1998**, *109*, 8218.
[72] S. Miertus, E. Scrocco, J. Tomasi, *Chem. Phys.* **1981**, *55*, 117.
[73] J. Tomasi, B. Mennucci, R. Cammi, *Chem. Rev.* **2005**, *105*, 2999.
[74] R. Seeger, J. A. Pople, *J. Chem. Phys.* **1977**, *66*, 3045.
[75] R. Bauernschmitt, R. Ahlrichs, *J. Chem. Phys.* **1996**, *104*, 9047.
[76] S. I. Gorelsky, AOMix: Program for Molecular Orbital Analysis, York University, Toronto, **1997**, http://www.sg-chem.net.
[77] S. I. Gorelsky, A. B. P. Lever, *J. Organomet. Chem.* **2001**, *635*, 187.

Received: April 2, 2009
Published Online: May 5, 2009

